BRIEF REPORT Open Access



Antagonistic regulation of LINE-1/Alu elements and their repressor APOBEC3B in cellular senescence

Daksha Munot¹, Yueshuang Lu¹, Isabell Haußmann¹, Gregoire Najjar², Charlotte Baur¹, Manvendra Singh³, Cagatay Günes², Daniel Sauter^{1*} and Ankit Arora^{4*}

Abstract

Long Interspersed Nuclear Elements-1 (LINE-1 or L1) make up approximately 21% of the human genome, with some L1 loci containing intact open reading frames (ORFs) that facilitate retrotransposition. Because retrotransposition can have deleterious effects leading to mutations and genomic instability, L1 activity is typically suppressed in somatic cells through transcriptional and post-transcriptional mechanisms. However, L1 elements are derepressed in senescent cells causing age-associated inflammation. Despite the recognition of L1 activity as a hallmark of aging, the underlying molecular mechanisms governing L1 derepression in these cells are not fully understood. In this study, we employed high throughput sequencing datasets and validated our findings through independent experiments to investigate the regulation of L1 elements in senescent cells. Our results reveal that both replicative and oncogene-induced senescence are associated with reduced expression of the cytidine deaminase *APOBEC3B*, a known suppressor of L1 retrotransposition. Consequently, senescent cells exhibited diminished levels of C-to-U editing of full-length L1 elements. Moreover, Ribo-seq profiling indicated that progression to senescence is not only associated with increased L1 transcription, but also translation of L1 ORFs. In summary, our results suggest that the depletion of APOBEC3B contributes to enhanced activity of L1 in senescent cells and promotion of L1-induced DNA damage and aging.

Keywords LINE-1, Alu, Senescence, Aging, APOBEC3B

Background

Almost half of the human genome consists of sequences derived from transposable elements (TEs) [1]). The majority of TE sequences belong to non-LTR retrotransposon families such as L1 (21% of the genome with \sim 500,000 copies) and Alu elements (\sim 10% of the genome with \sim 1 million copies) [2, 3]. While most L1 elements are inactive, a few full-length loci are still capable of retrotransposition [1]. Moreover, retrotransposon families that do not encode their own retrotransposition machinery (e.g. Alu and SVA elements) also exploit L1-encoded reverse transcriptase to integrate into new genomic loci [4, 5].



© The Author(s) 2025. **Open Access** This article is licensed under a Creative Commons Attribution-NonCommercial-NoDerivatives 4.0 International License, which permits any non-commercial use, sharing, distribution and reproduction in any medium or format, as long as you give appropriate credit to the original author(s) and the source, provide a link to the Creative Commons licence, and indicate if you modified the licensed material. You do not have permission under this licence to share adapted material erived from this article or parts of it. The images or other third party material in this article are included in the article's Creative Commons licence, unless indicated otherwise in a credit line to the material. If material is not included in the article's Creative Commons licence and your intended use is not permitted by statutory regulation or exceeds the permitted use, you will need to obtain permission directly from the copyright holder. To view a copy of this licence, visit http://creativecommons.org/licenses/by-nc-nd/4.0/.

^{*}Correspondence: Daniel Sauter Daniel.Sauter@med.uni-tuebingen.de Ankit Arora aankit@instem.res.in

¹Institute for Medical Virology and Epidemiology of Viral Diseases,

University Hospital Tübingen, Tübingen, Germany

²Department of Urology, Ulm University Hospital, Ulm, Germany

³Max Delbrück Center for Molecular Medicine in the Helmholtz Association (MDC), Berlin, Germany

⁴Institute for Stem Cell Science and Regenerative Medicine, Bengaluru,

Munot et al. Mobile DNA (2025) 16:39 Page 2 of 14

Due to the potential harmful effects of active TEs, such as insertional mutagenesis, the human genome has evolved independent mechanisms to suppress TEs at multiple steps of their retrotransposition cycle. For instance, specific KRAB-ZNFs recruit TRIM28 (Tripartite motif-containing protein 28) that silences L1 transcription elements by further recruiting chromatinmodifying enzymes such as the histone methyltransferase SETDB1 [6]. SETDB1 is also known to interact with the HUSH complex (TASOR, Periphilin, MPP8), causing long-term repression by perpetuating heterochromatin [7]. However, even if L1 elements are transcriptionally active, their retrotransposition can still be curbed at later steps. For instance, nucleases such as three prime repair exonuclease 1 (TREX1) prevent the accumulation of L1 transcripts [8, 9], while MOV10 decaps L1 RNA [10], thereby sequestering L1 ribonucleoprotein complexes in cytoplasmic aggregates [11]. A critical inhibition of retrotransposition is mediated by the members of the APOBEC (Apolipoprotein B mRNA Editing Catalytic Polypeptide-like) family of deaminases [12–20]. While APOBEC3 proteins are known to induce C-to-U mutations, leading to hypermutation, their role in suppressing L1 retrotransposition appears to extend beyond this deaminase activity [4]. Notably, overexpression of APO-BEC3A, B, C, and D inhibits L1 activity without corresponding increases in L1 point mutations, indicating a deaminase-independent mechanism [14]. Further supporting this, catalytically inactive mutants of APOBEC3B and C retain their ability to suppress L1 retrotransposition underscoring the multifaceted roles these proteins play in maintaining genomic stability [12, 16].

Despite these multilayered suppression mechanisms, L1 elements can be activated under certain conditions. For example, external stimuli such as ionizing radiation trigger L1 transcription [21]. Similarly, certain developmental stages are associated with increased L1 activity. These include early developmental stages such as embryonic cells that undergo epigenetic reprogramming and global demethylation [22]. Notably, DNA methylation of L1 repeats decreases with advancing age, and L1 activity has been proposed as a predictor of chronological age [23, 24]. In this case, L1 activity was shown to drive organismal aging and cellular senescence [25, 26]. Senescence describes a state of permanent cell-cycle arrest and resistance to apoptosis that can be induced by multiple intrinsic and extrinsic stimuli, including oncogene activation or genotoxic stress [27]. Genotoxic stress refers to DNA damage that can arise from various sources, including the activity of retrotransposons such as L1 elements, which induce double-strand breaks and disrupt genomic integrity through their insertion events. Senescence is typically associated with the release of inflammatory cytokines and other immune modulators, referred to as the senescence-associated secretory phenotype (SASP) [28]. These secreted factors can trigger the progression of proliferating, non-senescent cells to senescence [28].

The activation of L1 repeats in presenescent cells results in the production of nucleic acids that can activate cellular sensing pathways such as cGAS-STING or RIG-I, which mediate the production of type I IFN and ultimately SASP [25, 26, 29]. Hence, L1 activity in presenescent cells not only contributes to their transition to senescence, but can also induce a senescent state in bystander cells [30]. In addition to sensing of L1-derived nucleic acids, the retrotransposition and *de-novo* integration of L1 elements may promote senescence by triggering the vicious cycle of DNA damage, cell-cycle arrest and inflammation [26]. Overall, there is more than one way how uncontrolled activity of L1 can trigger cellular senescence.

While SASP is heterogenous, and numerous triggers of senescence have been described, L1 transcription has been observed in different types of senescence, including replicative senescence, oncogene-induced senescence and stress-induced premature senescence [25, 31]. L1 activation in senescent cells is associated with higher levels of accessible chromatin around the 5' UTR of L1 repeats [31]. Furthermore, the transcription factor PAX5 binds to the 5'-UTR of L1 and is proposed to contribute to their activation in cells entering senescence [32]. However, precise mechanism of enhanced L1 activity in (pre)senescent cells remains elusive, and the mechanisms underlying post-transcriptional L1 regulation are still unclear.

We hypothesized that the loss of various L1 controllers may result in L1 derepression at the transcriptional and/or post-transcriptional level. To investigate the expression dynamics of L1 and its repressors, we reanalyzed publicly available RNA-seq and Ribo-seq datasets from cells progressing to replicative or oncogene-induced senescence.

Our RNA-seq data analyses, together with validation experiments in fibroblasts, revealed that several L1 inhibitors, including the deaminase APOBEC3B, are downregulated in presenescent cells. In line with reduced APOBEC3B levels, we found evidence for decreased C-to-U editing and higher levels of L1 translation. In summary, our findings support a model in which reduced expression of restriction factors such as APOBEC3B contribute to increased L1 activity, ultimately leading to enhanced L1 cDNA sensing and potentially L1-mediated DNA damage in cells transitioning to senescence.

Materials and methods

Analysis of RNA-seq datasets from senescent cells

Raw RNA-seq reads from immortalized human primary BJ fibroblasts and ES-derived lung fibroblasts were

Munot et al. Mobile DNA (2025) 16:39 Page 3 of 14

obtained from [33] [GSE42509] and [25] [GSE109700], respectively. RNA-seq reads were mapped to the human (hg19) reference genome using STAR (v2.4.2a) [34]. We used STAR for its ability to detect novel splice junctions and as a non-canonical splice aligner for the detection of chimeric transcripts and circular RNA. Mapped reads were processed to obtain raw counts for gene expression estimation using featureCounts [35] from the subread package (v1.4.6). DESeq2 (v1.30.1) was used to process counts per million (CPM) and differential expression of genes in the R environment (v4.0.3). To determine the expression of cellular factors affecting L1 retrotransposition, we took advantage of a list of activators and suppressors of L1 retrotransposition previously identified in a genome-wide CRISPR/Cas9 screening [36], as well as experimentally validated and published L1 suppressors (Tables 1 and 2).

Analysis of repetitive elements

Mapping of RNA-seq reads to the human reference genome (hg19) was performed using bowtie (v1.0.1) [69] short read aligner with use of -N 1 and - -local parameters for effective alignment. FPKM values for expression were computed using cufflinks (v2.0.2) [70] with the usage of GTF file format for specific repetitive elements (L1 & Alu) obtained from the UCSC genome browser [71]. The annotation file of repetitive elements (L1 & Alu) was categorized into young, middle-aged and ancient sub-families.

Detection of APOBEC- and ADAR-edited RNA sites

A data analysis pipeline was designed, involving multiple rigorous iterations focused on the identification of APO-BEC- and ADAR-edited RNA sites within full-length L1 elements. Mapped RNA-seq reads were incorporated to perform local realignment, base-score recalibration, and candidate variant calling using the IndelRealigner,

Table 1 List of previously described L1 suppressors and their differential expression in replicative senescence

Symbol	BaseMean	log2FoldChange (Senescent vs. non-senescent)	IfcSE	stat	pvalue	padj	PMIDs
ADAR	13593.70544	-0.1767522525	0.1036717693	-1.704921732	0.08820902262	0.2020137145	[37, 38]
ADARB1	7923.720891	-1.135034549	0.230490103	-4.924439418	8.46E-07	5.84E-06	[37]
APOBEC3A	0.1771823279	-1.285752751	3.470979875	-0.3704293306	0.7110626231	0.8275012857	[17, 39–41]
APOBEC3B	207.4065383	-5.79319621	1.367403086	-4.23664117	2.27E-05	1.28E-04	[12–16]
APOBEC3C	1361.025833	0.2410312535	0.2173211663	1.109101601	0.2673863542	0.4647505347	[20]
APOBEC3F	51.2280652	0.4755750593	0.3508502683	1.355492933	0.1752605586	0.3414929439	[15, 20]
APOBEC3G	129.3980821	0.2909960237	0.6001933883	0.4848371032	6.28E-01	7.79E-01	[19], [42]
BRCA1	1407.430926	-4.512747793	0.1861865152	-24.23778	8.90E-130	2.98E-127	[43]
BRCA2	739.0177882	-4.747624492	0.3692232744	-12.85841067	7.71E-38	3.56E-36	[43, 44]
CDK12	2729.584381	-0.3958855794	0.07516753684	-5.266709487	1.39E-07	1.05E-06	[43, 45]
ERCC1	2590.195369	-0.5402738228	0.1691851287	-3.193388373	0.001406136906	0.005646594775	[46-48]
FANCA	859.0160672	-4.567728483	0.2331840498	-19.58851168	1.94E-85	3.27E-83	[29, 46]
FANCC	576.3773425	-1.160195003	0.1955136277	-5.934087647	2.95E-09	2.69E-08	[43, 45, 49]
FANCD2	1704.582755	-4.578016147	0.3447290095	-13.28004322	3.02E-40	1.51E-38	[29, 46]
FANCI	2634.783325	-3.87242164	0.1598756147	-24.22146521	1.32E-129	4.39E-127	[43-45, 49]
MCM2	3296.152558	-3.886187297	0.1677845159	-23.16177555	1.11E-118	3.17E-116	[50]
MEN1	630.8288085	-0.4623118186	0.1703850649	-2.713335344	6.66E-03	2.26E-02	[43–45, 49, 51]
MORC2	1785.005624	-0.4624012188	0.1333309595	-3.468070886	5.24E-04	2.32E-03	[36, 52]
MOV10	2327.601271	-0.4614617449	0.1198897	-3.849052463	1.19E-04	5.92E-04	[10, 53]
PPHLN1	2641.473683	-0.1631561449	0.1763207885	-0.9253369741	3.55E-01	5.62E-01	[54, 55]
RNASEH2A	1237.108977	-3.591983858	0.133416489	-26.92308789	1.18E-159	6.70E-157	[56, 57]
RNASEH2C	684.8608255	-0.699231256	0.2099357848	-3.330691129	0.000866306685	0.003662943363	[50, 57–61]
SAFB	2054.418039	-1.028261863	0.1528576456	-6.726924643	1.73E-11	1.95E-10	[50, 58–61]
SETDB1	1429.963425	-0.3200143374	0.15809441	-2.024197677	4.29E-02	1.13E-01	[62–66]
SLFN5	5495.230925	1.451515478	0.1754247483	8.274291354	1.29E-16	2.17E-15	[50, 58–60]
SLX4	588.5899453	-1.274654754	0.1839240204	-6.930333247	4.20E-12	5.03E-11	[29, 46]
TASOR	4660.656721	0.1989861321	0.12541377	1.586637034	1.13E-01	0.2441933186	[36, 52, 54, 67, 68]
TRIM5	1484.227229	-0.4452832903	0.1658357538	-2.685086178	0.007251110699	0.02432820151	[50, 58, 59]
TRIM28	10838.28195	-1.505814595	0.2386464441	-6.309813672	2.79E-10	2.82E-09	[50, 58]

Munot et al. Mobile DNA (2025) 16:39 Page 4 of 14

Table 2 List of previously described L1 suppressors and their differential expression in oncogene-induced senescence

Symbol	BaseMean	log2FoldChange (Senescent vs. non-senescent)	IfcSE	stat	pvalue	padj	PMID
ADAR	8368.720992	-0.0952368314	0.3484200601	-0.2733391165	0.7845925491	0.9379457021	[37, 38]
ADARB1	784.1280316	-1.794027878	0.4824583062	-3.718513818	0.0002003983319	0.004907446132	[37]
APOBEC3B	310.1567351	-6.752480232	0.9267465089	-7.286221386	3.19E-13	4.08E-11	[12–16]
APOBEC3C	1932.589211	1.042916509	0.3744387161	2.785279577	5.35E-03	6.49E-02	[20]
APOBEC3F	96.05824889	-1.044669274	0.5519057116	-1.892840121	5.84E-02	0.3284414554	[15]
APOBEC3G	58.77648727	-1.272260731	0.7374265801	-1.725271051	0.08447863646	0.4083211076	[15, 19, 42]
BRCA1	1153.869341	-3.293584005	0.390952605	-8.42450968	3.62E-17	7.06E-15	[43]
BRCA2	638.2982856	-4.015285616	0.4324966275	-9.283969772	1.63E-20	4.09E-18	[43, 44]
CDK12	3317.522914	0.04627908005	0.3399569552	0.136132176	0.8917167915	0.9751049779	[45]
ERCC1	2786.928375	1.293056276	0.3783880289	3.417275856	0.0006325115405	0.0126031845	[46-48]
FANCA	1279.213077	-4.675477182	0.4690577733	-9.967806629	2.11E-23	6.35E-21	[29, 46]
FANCC	277.9076235	-1.782393688	0.5618803281	-3.172194504	0.001512916418	0.02486001012	[43, 45, 49]
FANCD2	829.1968194	-4.839139327	0.4218704277	-11.4706768	1.85E-30	9.82E-28	[29, 46]
FANCI	2143.908685	-3.427379534	0.3631840345	-9.43703249	3.83E-21	9.78E-19	[43-45, 49]
MCM2	3052.158556	-3.440282643	0.4890269477	-7.034955148	1.99E-12	2.42E-10	[50]
MEN1	1266.918142	-0.1952086275	0.3569306757	-0.54690908	5.84E-01	9.14E-01	[43-45, 49, 51]
MORC2	1392.51223	-0.09762543581	0.34667252	-0.2816070792	0.7782448114	0.9368147665	[36, 52]
MOV10	1887.955436	0.0634066136	0.3514920582	0.1803927347	0.8568442577	0.9660164808	[10, 53]
PPHLN1	1367.840596	0.4616055898	0.4073374611	1.133226462	2.57E-01	7.20E-01	[54, 55]
RNASEH2A	1406.277496	-3.624748877	0.4825712269	-7.51132408	5.85E-14	8.21E-12	[56, 57]
RNASEH2C	793.4435244	0.2589269923	0.3757228108	0.6891436583	4.91E-01	8.96E-01	[50, 57–61]
SAFB	2466.688488	-1.186810605	0.4269607716	-2.779671303	0.005441394536	0.06559601113	[50, 58–61]
SETDB1	724.7476742	-0.3170419275	0.371907219	-0.8524758633	0.3939500299	0.8434003343	[62–66]
SLFN5	4231.544048	1.199170999	0.712351448	1.683397994	0.09229807134	0.4295928367	[50, 58–60]
SLX4	896.9424992	-0.3033578976	0.420107135	-0.7220965137	0.4702351415	0.8843501764	[29, 46]
TASOR	2524.530699	-0.3932232306	0.4047780991	-0.97145382	3.31E-01	7.98E-01	[36, 52, 54, 67, 68]
TRIM5	759.3398736	-1.336946212	0.3767997659	-3.54816094	0.0003879311041	0.008439967853	[50, 58, 59]
TRIM28	11634.48129	-1.256029245	0.3900891791	-3.219851542	0.001282569985	0.02184652445	[50, 58]

TableRecalibration and UnifiedGenotyper tools with the parameters stand call conf to 0 and stand emit conf to 0 and the output mode set to EMIT ALL CONFIRMED SITES from the Genome Analysis Toolkit (GATK) (v3.5-0) [36, 72]. In addition, some iteration steps of the SNPiR pipeline [73] were adapted, and obtained variants were subjected to it. The intended variants were incorporated into different filtering steps to obtain true variants by removing false-positive variant calls. First, variants with quality up to 20 were filtered. Then, the mismatches at the 5' ends of the reads were removed in this step. Furthermore, the obtained variants were directed to filter in L1 elements. Shell scripting and bedtools [74] were used to retrieve the edited sites for each sample across full-length L1 elements. The obtained editing sites for each sample were further filtered for C to U mutations for APOBEC editing sites and A to I mutations for ADAR editing sites.

Estimation of L1 encoded proteins

The repeat masker track for L1 elements was downloaded from the UCSC genome browser. More specifically,

only full-length L1 elements were extracted from this track, and a BED file was prepared. Ribosomal profiling (Ribo-seq) samples for immortalized human primary BJ fibroblasts were obtained from [33] [GSE42509]. Adapter sequences were removed from the raw FASTQ reads, and ribosomal sequences were eliminated using quick alignment with TopHat2 [75]. Unmapped reads from this alignment were converted into FASTQ format using bam2fastx [75]. The consensus sequence for fulllength L1 elements was constructed by converting the BED file into FASTA format with fastaFromBed [74]. These consensus sequences were aligned to Ribo-seq reads (single-end, 50 bp) using Bowtie (v1.0.1) using the best parameter, across conditions of proliferation and senescence. Uniqueness for 35-mers and alignability for 36-mers with respect to full-length L1 elements in the Ribo-seq data were computed. Normalized coverage for uniquely mapped reads was obtained using bamCoverage for each condition. Further, computation of matrix was performed on the bigwig file of each condition by using computeMatrix [76].

Munot et al. Mobile DNA (2025) 16:39 Page 5 of 14

Transduction of BJ cells

BJ cells and HEK293T cells were purchased from ATCC (ATCC LGC Standards GmbH, Manassa, Virginia, USA; cat# CRL-2522 and CRL-3216, respectively). BJ-hTERT cells were generated by transduction with the pWZL-Blast-Flag-HA-hTERT retroviral vector (addgene; cat.# 22396). All cells were cultured in DMEM high glucose, penicillin (10.000 unit/mL), streptomycin (10 mg/mL), and 10% FCS at 37 °C and 5% CO2. HEK293T cells were transfected with PWZL-Hygro-H-Ras^{G12V} using PEI. On the following day, the cell culture medium was changed and 24 h later a supernatant containing the viral particles was filtered through a 0.45 µm filter. Viral supernatant and 8 µg/µL polybrene were then added to the target cells (primary BJ and immortalized BJ-hTERT) for 24 h. Lastly, cells were washed three times with DPBS and appropriate selection antibiotic was added.

gRT-PCR

For BJ cells, total RNA was isolated 7 days post-transduction (d.p.t.), using the RNeasy Mini Kit (Qiagen, cat# 74106) following the manufacturer's instructions. For HEK293T cells, total RNA was isolated 2 days post etoposide stimulation using the RNeasy Plus Mini Kit (Qiagen # 74136) according to the manufacturer's instructions. RNA quality and quantity were assessed using a spectrophotometer. Reverse transcription was performed using the PrimeScript RT Reagent Kit (Perfect Real Time) (TAKARA, cat# RR037A) with oligo dT primers and random hexamers. Quantitative real-time PCR (qPCR) was conducted using specific primer/probe sets for APOBEC3A (forward): 5'-GAGAAGGGACAAGCA CATGG-3', (reverse): 5'-TGGATCCATCAAGTGTCT GG-3'; APOBEC3B human probe: (Thermo Fisher, cat# Hs00358981_m1); APOBEC3C (forward): 5'-AGCGCTT CAGAAAAGAGTGG-3', (reverse): 5'-AAGTTTCGTT CCGATCGTTG-3'; APOBEC3F (forward): 5'-CCGTTT GGACGCAAAGAT-3', (reverse): 5'-CCAGGTGATCTG GAAACACTT-3'; APOBEC3G (forward): 5'-CCGAGGA CCCGAAGGTTAC-3', (reverse): 5'-TCCAACAGTGCT GAAATTCG-3'; CDKN1A/p21 human probe: (Thermo Fisher, cat# Hs00355782_m1), with GAPDH (forward): 5'-CCGAGGACCCGAAGGTTAC-3'; (reverse): 5'-TCC AACAGTGCTGAAATTCG-3', human probe: (Thermo Fisher, cat# Hs02786624_g1) serving as the internal control. Each sample was analyzed in technical triplicates.

Western blot

To validate over-expression of APOBEC3B, transfected HEK293T cells were washed with PBS and lysed in Western blot lysis buffer (150 mM NaCl, 50 mM HEPES, 5 mM EDTA, 0.1% NP40, 500 μ M Na3VO4, 500 μ M NaF, pH 7.5), followed by centrifugation at 20,800 xg for 20 min at 4 °C. Lysates were then mixed with loading

buffer containing 10% β -mercaptoethanol and heated at 95 °C for 5 min. Proteins were separated on NuPAGE 4–12% Bis–Tris Gels, transferred onto Immobilon-FL PVDF membranes, and probed with primary antibodies: anti-HA tag (abcam, catalog number: ab18181), and anti-GAPDH (BioLegend, catalog number: #607902). After washing, membranes were incubated with secondary antibodies labeled with infrared dyes (LI-COR IRDye). Protein bands were detected using a LI-COR Odyssey scanner.

L1 reporter assay

The retrotransposition-competent L1-GFP reporter plasmid (99 PUR L1RP EGFP, "wt") and the retrotransposition-defective negative control plasmid (99 PUR JM111 EGFP, "mut.") were previously described by Ostertag et al. [77]. Both constructs harbor a CMV-driven eGFP reporter cassette that includes an intron inserted in the reverse orientation within the 3' UTR. Expression of eGFP serves as an indicator of successful retrotransposition, as it requires splicing, reverse transcription, and genomic integration to become active. HEK293T cells (cultured in DMEM, penicillin (100 unit/mL), streptomycin (100 μ g/mL), and 10% FCS at 37 °C and 5% CO₂) were co-transfected with the L1 reporter plasmid and either an APOBEC3B expression vector (pcDNA3.1, 3x HA-tag) or an empty control vector (pcDNA3.1) at a 3:1 molar ratio using calcium phosphate. An expression plasmid for IFI16 (pCG, HA-tag) served as positive control [78]. One day post transfection, half of the cells were treated with 0.2 µM etoposide to induce a senescence-like phenotype. Two days post transfection, 2.5 µg/ml puromycin was added to select cells harboring the L1 reporter plasmid. Four days later, the percentage of GFP-positive cells was quantified by flow cytometry.

Statistical analysis

Wilcoxon-Mann-Whitney test, paired t-test and Ordinary one-way ANOVA test were used for analysis at the transcriptional and translational level. *p*-values < 0.05 were considered statistically significant.

Results

Replicative and oncogene-induced senescence are associated with decreased expression L1 repressors such as APOBEC3B

While L1 activity was shown to be upregulated in senescence [25, 31], the mechanisms underlying L1 activation remained poorly understood. We therefore commenced this study by determining the expression levels of known L1 suppressors in primary human lung fibroblasts transitioning from a proliferative state to early and ultimately late replicative senescence. By leveraging a previously published RNA-seq dataset [25] [GSE109700], we

Munot et al. Mobile DNA (2025) 16:39 Page 6 of 14

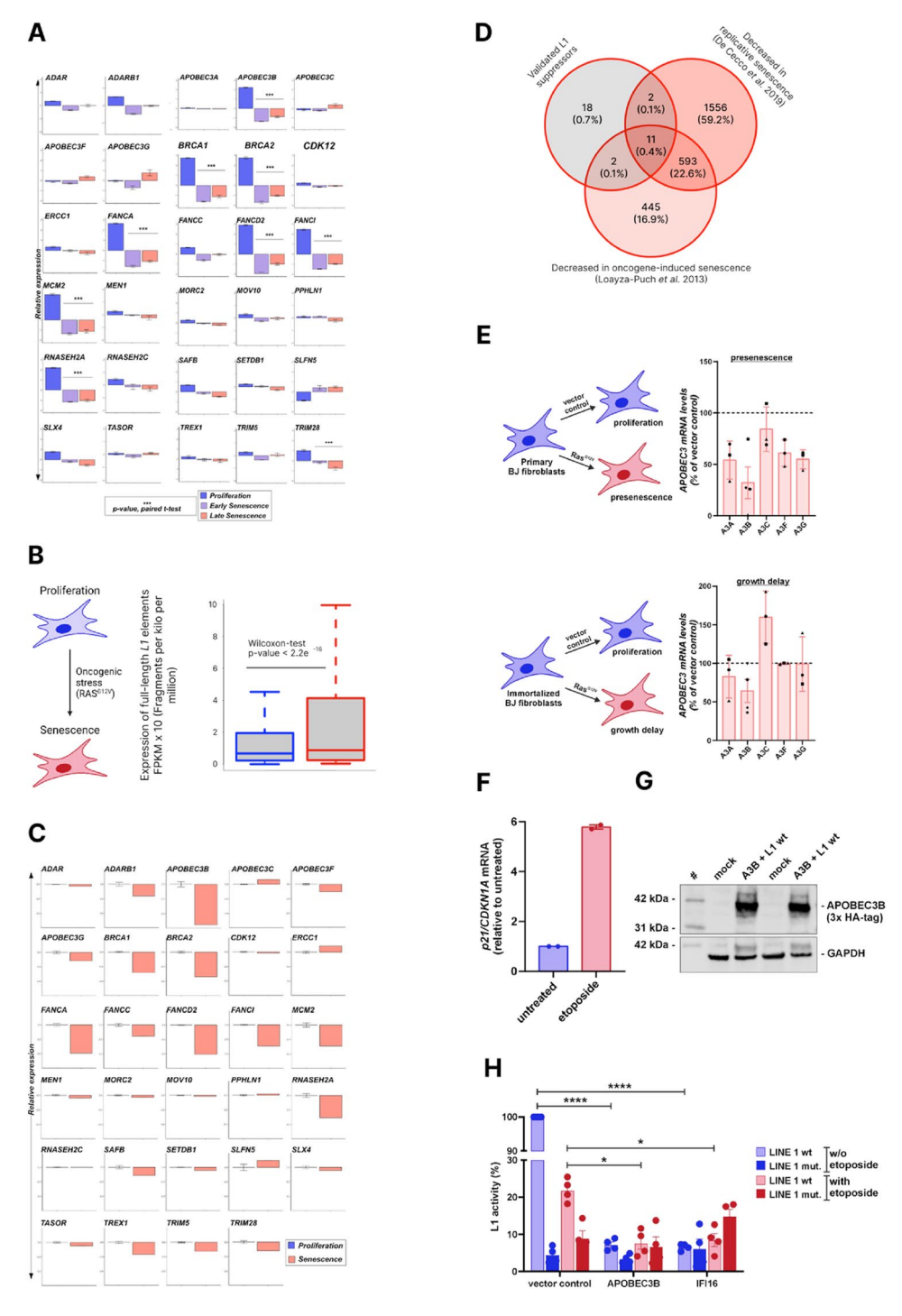


Fig. 1 (See legend on next page.)

Munot et al. Mobile DNA (2025) 16:39 Page 7 of 14

(See figure on previous page.)

Fig. 1 Decreased expression of L1 repressors in senescent cells. A Expression of known L1 suppressors in human lung fibroblasts transitioning from a proliferative state to early and late replicative senescence (see also Table 1). Expression relative to the mean of all three conditions is shown. A paired t-test was performed to determine statistically significant differences between proliferating and senescent (early+late) cells (***p < 0.001). B Expression of fulllength L1 elements is significantly increased in senescent vs. proliferating cells (p-value < 2.2e-16). C Expression of known L1 suppressors in BJ fibroblasts before and after RAS^{G12V}-mediated induction senescence. The analyses in (A, B, and C) are based on publicly available RNA-seq datasets (GSE109700 and GSE42509, respectively). **D** Venn diagram illustrating the overlap of known L1 suppressors with genes that are down-modulated during transition to replicative and/or oncogene-induced senescence. **E** Cartoons illustrating the transduction process of BJ fibroblast cells with empty or RAS^{G12V} expressing vectors shown on the left. Primary BJ cells expressing RAS^{G12V} enter a presenescent state, while hTERT-immortalized cells undergo a transient growth delay, Bar graphs on the right show APOBEC3A, B, C, F and G mRNA levels upon transduction with lentiviruses encoding RASG12V and normalization to cells transduced with the vector control. F HEK293T cells were stimulated with 0.2 µM etoposide. Two days later, cells were harvested, and p21/CDKN1A expression was analyzed by qPCR (G, H) HEK293T cells were co-transfected with intact (wt) or mutated (mut.) L1 GFP reporter constructs, together with the indicated expression plasmids. One day later, cells were stimulated with etoposide or left untreated. **G** Expression of APOBEC3B was validated by Western blotting two days post transfection. One exemplary Western blot out of two is shown, **H** Six days post transfection, the percentage of GFP positive cells was determined by flow cytometry as a reporter for L1 retrotransposition. Values were normalized to the L1 wt control without etoposide and without overexpression of APOBEC3B/IF116. Mean values of two to four independent experiments ± SEM are shown in panels (E), (F) and H. (*p < 0.05; ****p<0.0001)

compared the expression of L1 suppressors in proliferative cells relative to both early and late senescent cells taken together. We found 13 L1 repressors to be significantly downregulated in senescent cells compared to proliferating cells (Fig. 1A; Table 1). The five most strongly reduced transcripts encode for the deaminase APO-BEC3B (log2fc -5.79 & adjusted p-value 1.28e-04) and the DNA repair proteins BRCA2 (log2fc -4.75 & adjusted p-value 3.56e-36), FANCD2 (log2fc -4.58 & adjusted p-value 1.51e-38), FANCA (log2fc -4.57 & adjusted p-value 3.27e-83) and BRCA1 (log2fc -4.51 & adjusted p-value 2.98e-127) (Table 1). In contrast, only a single L1 suppressor, SLFN5, was significantly upregulated during progression to senescence (log2fc 1.45 & adjusted p-value 2.17e-15) (Table 1). The data suggest that progression to senescence is marked by a significant downregulation of multiple L1 suppressors, particularly APOBEC3B, BRCA2, FANCD2, FANCA, and BRCA1, while SLFN5 is the only L1 repressor significantly upregulated.

To determine whether a similar expression pattern of L1 inhibitors can also be observed in other models of senescence, we determined their expression in cells undergoing oncogene-induced senescence [25]. To this end, we re-analyzed RNA-seq data obtained from immortalized human BJ primary fibroblasts [GSE42509], in which senescence was induced by tamoxifen-inducible expression of the oncogenic RAS^{G12V} gene [33]. Since this study did not monitor the activity of transposable elements, we first analyzed the transcription of L1 elements in this data set. As observed for replicative senescence, L1 expression in BJ fibroblasts was significantly elevated upon Ras^{G12V}-mediated induction of oncogenic senescence (Fig. 1B). Furthermore, oncogene-induced senescence was also associated with a significant decrease in the expression of L1 inhibitors (Fig. 1C; Table 2). Intriguingly, eleven L1 repressors were significantly depleted in both data sets (Tables 1 and 2; Fig. 1D). In oncogene-induced senescence, the five most strongly depleted transcripts were APOBEC3B (log2FC -6.75 & adjusted p-value 4.08e-11), FANCD2 (log2FC -4.84 & adjusted p-value 1.51e-38), FANCA (log2FC -4.68 & adjusted p-value 6.35e-21), BRCA2 (log2FC -4.02 & adjusted p-value 4.09e-18) and RNASEH2A (log2FC -3.62 & adjusted p-value 8.21e-12) (Fig. 1C; Table 2). Again, expression of SLFN5 was modestly increased in senescent vs. proliferating cells (log2FC 1.20 & adjusted p-value 0.43). These findings indicate that both replicative and oncogene-induced senescence are marked by a significant downregulation of multiple L1 inhibitors.

Next, we expanded our analyses to a list of potential L1 regulators identified by Liu and colleagues [36]. While the activity of many of the identified activators and inhibitors remains to be experimentally validated, the candidate L1 regulators are the results of unbiased genome-wide CRISPR screens [36]. Several L1 suppressors were down-regulated in cells progressing from proliferation to senescence (Fig. 2). This was particularly evident for cells undergoing replicative senescence (Fig. 2B). Surprisingly, several L1 activators also showed reduced expression in cells transitioning to (replicative) senescence (Fig. 2C, D).

Since APOBEC3B was the most strongly down-regulated repressor in both replicative and oncogene-induced senescence (Fig. 1A, C; Tables 1 and 2), we validated its differential expression via qRT-PCR. Related APOBEC3 gene family members were included as additional controls. We took advantage of the Ras^{G12V} fibroblast model, including telomerase reverse transcriptase (hTERT) positive and negative cells. As previously described [79, 80], hTERT-negative BJ cells show signatures of premature senescence 7 days post transduction with Ras^{G12V}. In contrast, hTERT-immortalized BJ fibroblasts do not enter senescence, but stay in a growth-delayed state between 7 and 14 days after Ras^{G12V} expression that is ultimately overcome [68, 80] (Fig. 1E, left). 7 days after Ras^{G12V} expression, APOBEC3B levels decreased by 68% in presenescent, telomerase-negative cells. In contrast, a 36% reduction of APOBEC3B expression was observed in hTERT-expressing cells (Fig. 1E, right). In line with

Munot et al. Mobile DNA (2025) 16:39 Page 8 of 14

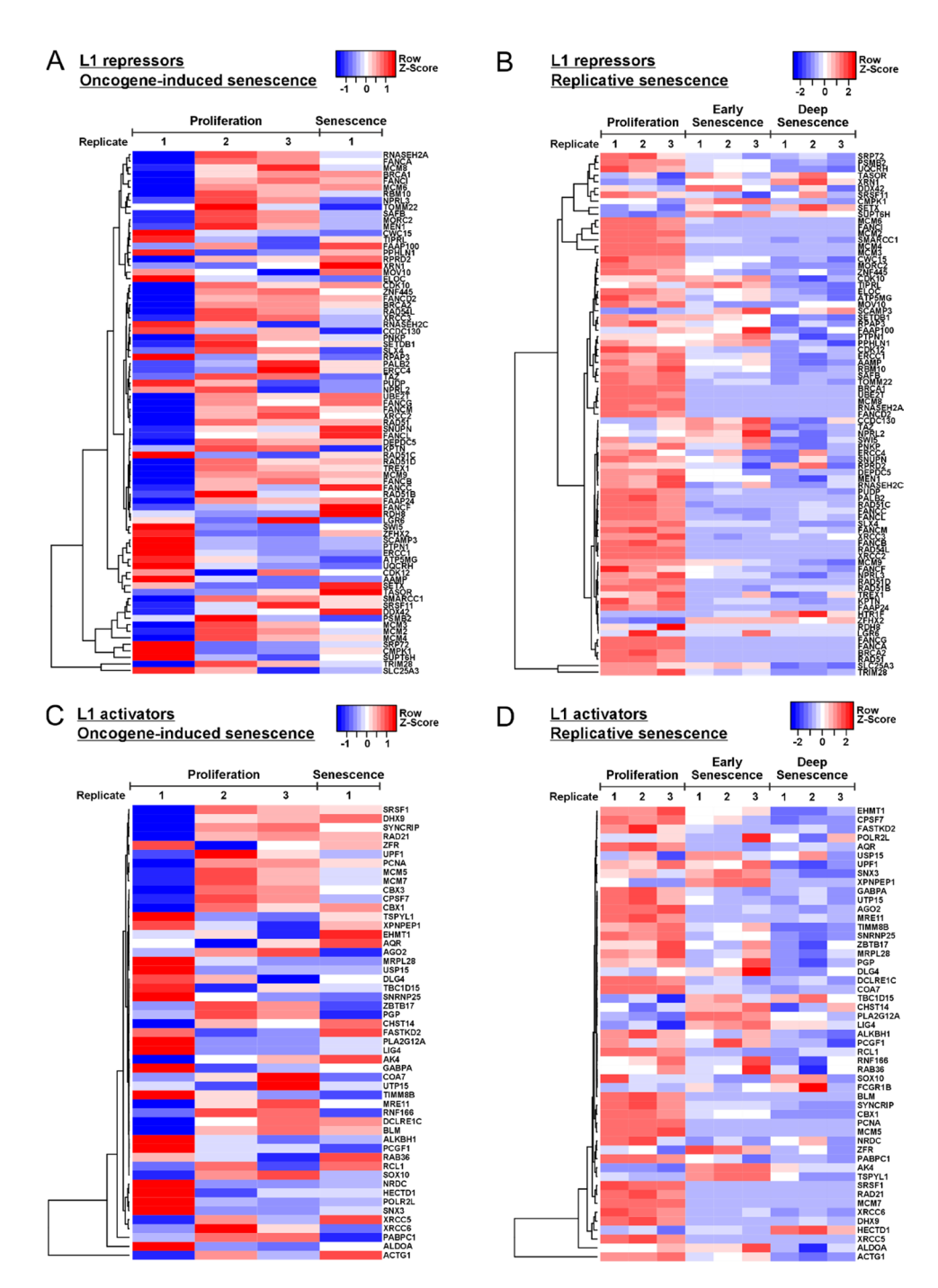


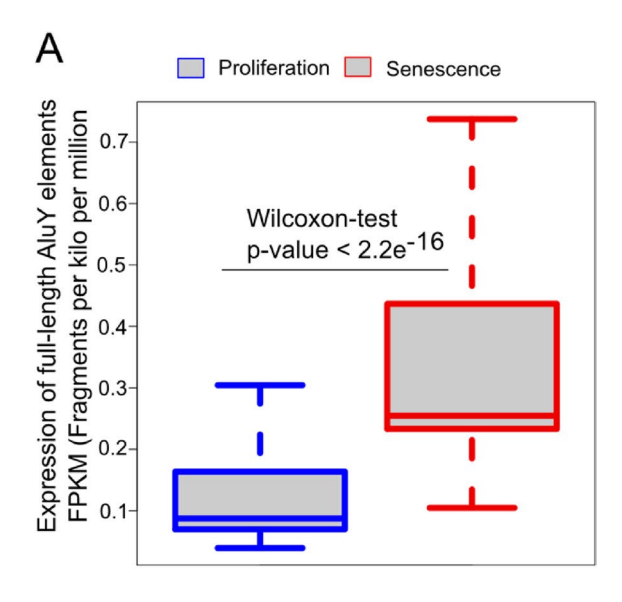
Fig. 2 Differential expression of L1 regulators in senescent vs. proliferating cells. A-D Heatmaps illustrate the differential expression of (A, B) L1 suppressors and (C, D) L1 activators identified in a CRISPR/Cas screen by Liu and colleagues [36] in senescent vs. proliferating cells. Data were obtained from cells undergoing (A, C) oncogene-induced senescence [33] or (B, D) replicative senescence [25]

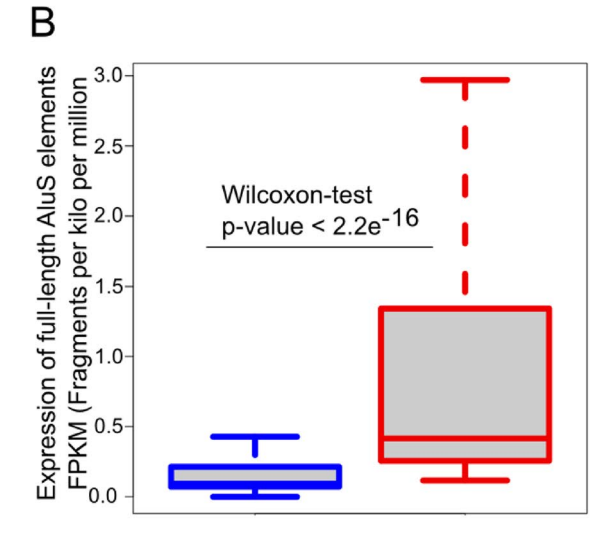
the RNA-seq results (Fig. 1C), the mRNA levels of *APO-BEC3A*, *C*, *D*, *F*, and *G* were reduced to a lesser degree or remained unchanged.

To test whether APOBEC3B is in principle able to restrict L1 activity in senescent cells, we took advantage of a previously described GFP reporter system [77] that enables monitoring of L1 retrotransposition in the presence or absence of ectopically expressed restriction

factors. Briefly, HEK293T cells were co-transfected with the L1-GFP reporter construct or a transposition-defective mutant thereof, together with an expression plasmid for APOBEC3B. One day later, the cells were treated with etoposide to induce a senescence-like state [77, 81]. Expression of the senescence marker *p21/CDKN1A* and APOBEC3B were determined by qPCR and Western blot, respectively (Fig. 1F, G). The previously described L1

Munot et al. Mobile DNA (2025) 16:39 Page 9 of 14





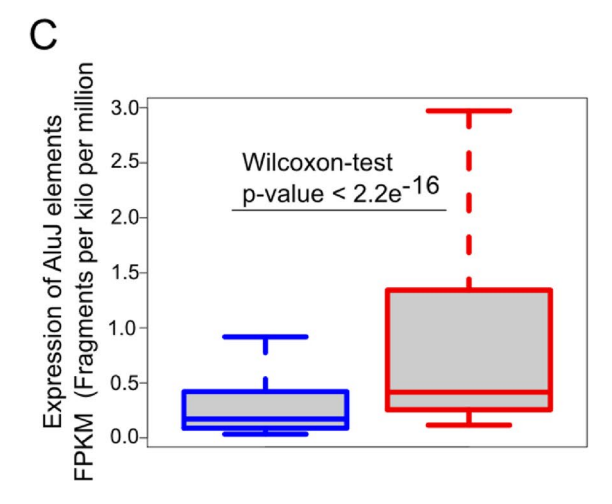


Fig. 3 Expression of Alu elements is significantly increased in senescent vs. proliferating cells. **A-C** Expression of **(A)** AluY, **(B)** AluS and **(C)** AluJ elements in human BJ primary fibroblasts transitioning from a proliferating state to RAS^{G12V}-induced senescence [33]. *p*-values were calculated using the Wilcoxon-Mann-Whitney test

inhibitor IFI16 served as positive control [78]. Quantification of GFP expression via flow cytometry revealed that APOBEC3B and IFI16 are able to restrict L1 not only in proliferating, but also in etoposide-treated cells (Fig. 1H).

Together with the RNA-seq and qPCR data described above, these findings demonstrate that APOBEC3B is a potent suppressor of L1, but expressed to lower levels during transition of proliferating cells to oncogene-induced and replicative (pre)senescence.

Expression of Alu element subfamilies is increased in senescent cells

Many L1 repressors also restrict other transposable elements. For example, APOBEC3 family members, including APOBEC3B [16, 19, 27, 42, 82, 83], also suppress Alu retrotransposition, and a subset of Alu repeats is bound by TRIM28 [27, 82]. We therefore expanded our analyses to different Alu elements, which belong to the group of short interspersed nuclear elements (SINEs). These include the two major Alu subfamilies AluJ and AluS [84], as well as AluY, a sub-subfamily of AluS [85]. Expression of all three Alu subfamilies was higher in oncogene-induced senescent cells compared to proliferating cells (*p*-values < 2.2e-16) (Fig. 3). These results demonstrate that reduced expression of TE suppressors is not only associated with increased L1 activity, but also with increased expression of the major Alu subfamilies.

Senescent cells show reduced signatures of APOBEC-induced L1 RNA editing

APOBEC3B, the most strongly downregulated repressor in senescent vs. proliferating cells (Fig. 1A, C; Tables 1 and 2), is able to deaminate both RNA and DNA [86]. Although APOBEC3 proteins are able to restrict L1 independently of their deaminase activity [14, 15, 20], we therefore hypothesized that the reduction of APO-BEC3B expression may coincide with decreased RNA editing in cells transitioning to senescence. To test this hypothesis, we examined APOBEC3-mediated RNA editing profiles in cells progressing to oncogene-induced senescence [33]. We employed RNA-seq datasets for identification of RNA editing profiles. We incorporated mapped RNA-seq reads to execute local realignment, base-score recalibaration and candidate variant calling by using GATK toolkit. The obtained variants were incorporated to into various filtering steps to obtain true

Munot et al. Mobile DNA (2025) 16:39 Page 10 of 14

variants by removal of false-positive variant calls. Furthermore, the obtained variants were directed to filter in L1 elements. Using an in-house pipeline, we retrieved edited sites for each sample across full-length L1 elements (see Methods). When investigating the loci of ancient (e.g. L1PA6, L1PA7) and middle-aged L1 subfamilies (e.g. L1PA2, L1PA3, L1PA4, L1PA5), which are not capable of retrotransposition, we observed no significant difference in the editing frequency between proliferating and senescent cells (Fig. 4A). In contrast, the evolutionary youngest and most active L1 subfamilies (e.g. L1Hs, L1PA1) showed an ~ 8 fold reduced editing frequency in senescent vs. non-senescent cells (Fig. 4B) (p-value = 0.024). As additional control, we also monitored editing signatures induced by ADAR (Adenosine Deaminase Acting on RNA) proteins, which convert adenosine into inosine [87]. ADAR1 and ADAR2 (= ADARB1) both restrict L1 [37, 38], and ADARB1 was significantly downregulated in senescent vs. non-senescent cells (Tables 1 and 2). However, we found no significant changes in ADAR-mediated editing signatures within L1 elements (Fig. 4C, D). In summary, our RNA editing analyses point towards a reduced mutagenic activity of at least one APOBEC3 protein in senescent cells.

Translation of L1 ORFs is increased in senescent cells

Increased L1 transcription and decreased L1 RNA editing in senescent cells are predicted to result in increased translation of L1 ORFs. We therefore examined publicly available Ribo-seq datasets of immortalized human primary fibroblasts in proliferative and senescent (oncogene-induced) states [33]. Due to the short sequencing reads (29–35 bps), the analysis of Ribo-seg datasets for TEs, especially the youngest ones, poses major alignability and mappability challenges [88]. To overcome these challenges, we aligned the Ribo-seq datasets with the full length L1 consensus sequence using an in-house pipeline and compared it to the genome-wide 35 bps unique mappability/alignability of full-length L1 elements. After calculating Ribo-seq coverage (see Methods), we were able to identify a few hundred mappable reads over the full-length L1 consensus sequence comprising both ORFs with a similar pattern of 35 bps mappability over different L1 elements (Fig. 4E). As expected, stronger signals were observed around the translation start sites (TSS) and translation end sites (TES), where ribosomes briefly pause at the start and stop codons, respectively (Fig. 4F). Taken together, the results demonstrate that progression to senescence is not only associated with increased transcription, but also increased translation of L1 elements.

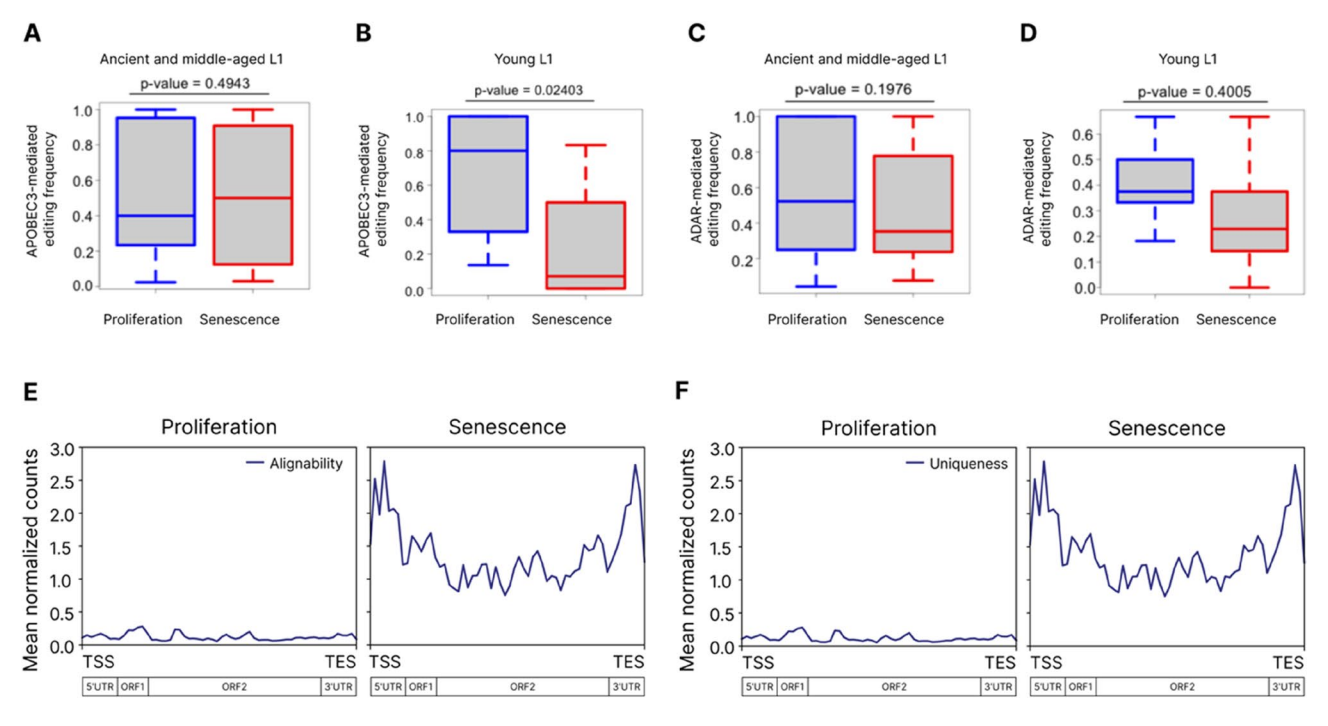


Fig. 4 Editing and translation of L1 RNA in senescent vs. proliferating cells. **A** Frequency of APOBEC3-mediated editing of ancient (e.g. L1PA6, L1PA7) and middle-aged (e.g. L1PA2, L1PA3, L1PA4, L1PA5) L1 subfamilies. **B** Frequency of APOBEC3-mediated editing of the youngest L1 loci (e.g. L1HS), which are still capable of retrotransposition (*p*-value = 0.02403). **C** Frequency of ADAR-mediated editing of ancient (e.g. L1PA6, L1PA7) and middle-aged (e.g. L1PA2, L1PA3, L1PA4, L1PA5) L1 subfamilies. **D** Frequency of ADAR-mediated editing of the youngest L1 loci (e.g. L1HS). Statistically significant differences in editing frequency were calculated using the Wilcoxon-Mann-Whitney test. The analyses in (**A-D**) are based on publicly available RNA-seq datasets (GSE42509. (**E**) & (**F**) Coverage-plot demonstrating the enrichment of Ribo-seq reads within L1 in senescence vs. proliferation. While (**E**) describes the enrichment for alignability, (**F**) describes the enrichment for uniqueness. Analyses in (**E**) and (**F**) are based on Ribo-seq datasets obtained from [33]

Munot et al. Mobile DNA (2025) 16:39 Page 11 of 14

Discussion

Our study provides insights into the expression dynamics of TE regulators in presenescent and senescent cells that may enable the derepression of L1 and/or Alu elements and ultimately contribute to an irreversible cell cycle arrest and inflammaging. By analyzing publicly available RNA-seq datasets, we reveal a consistent decrease in the expression of various TE inhibitors in two major subtypes of senescence, i.e. replicative and oncogeneinduced senescence. Vice versa, several TE activators are upregulated in (pre)senescent cells. These expression changes of TE modulators are tightly coupled with increased transcription and/or translation of L1 and Alu elements. Thus, our findings suggest that a major dysregulation of TE-regulating factors contributes to L1 and Alu derepression in cells transitioning from a proliferating to a senescent state.

Among the commonly down-regulated inhibitors were transcriptional repressors such as TRIM28/KAP1, DNA replication regulators such as MCM2, but also several RNAses (e.g. RNASEH2A) and DNA repair proteins (e.g. FANCA, FANCD2, FANCC, FANCI, BRCA1, BRCA2) (Fig. 1A, C; Tables 1 and 2). The most strongly downregulated L1 repressor was APOBEC3B. This deaminase is well known for its ability to restrict exogenous retroviruses such as HIV by inducing lethal hypermutations in the viral genome [89]. While it also restricts L1 elements, this inhibitory activity is independent of RNA editing [90]. Still, we observed signatures of APOBEC3-mediated editing of L1 transcripts. Notably, the exact mechanisms underlying APOBEC3-mediated L1 restriction have remained largely unclear. There is no correlation between the subcellular localization of individual APOBEC3 proteins and their ability to restrict L1, although L1 reverse transcription occurs in the nucleus [14, 16]. Similarly, the activity of APOBEC3 proteins to restrict L1 does not correlate with their ability to restrict HIV-1 lacking the APOBEC3 antagonist vif [16, 20]. Mutational analyses identified E68 as a residue involved in APOBEC3B-mediated L1 inhibition, also in the absence of any deaminase activity [16]. Bogerd and colleagues speculated that this residue may be involved in the interaction with L1 ribonucleoprotein complexes [16]. Indeed, co-immunoprecipitation experiments revealed a potential interaction of APOBEC3B with the L1 ORF1 protein [13].

In our analyses, APOBEC3B was the most strongly down-modulated member of the APOBEC3 family in both oncogene-induced and replicative senescence (Tables 1 and 2), strongly suggesting that it is likely the principal contributor to the observed L1 editing and suggesting a shared regulatory mechanism which in turn driving L1 activation in senescence. One interesting aspect in this context is that in contrast to other

APOBEC3 genes, *APOBEC3B* is not IFN-inducible [91]. Thus, its expression is not expected to be increased upon L1-mediated IFN production.

Our analysis of RNA editing profiles in cells progressing to oncogene-induced senescence revealed distinct patterns among L1 subfamilies. Specifically, the evolutionarily youngest and most active L1 subfamilies, such as L1HS and L1PA1, exhibited approximately a~8 fold reduction in editing frequency in senescent cells compared to non-senescent cells (Fig. 4B). In contrast, no significant differences in editing frequency were observed at loci corresponding to ancient (e.g., L1PA6, L1PA7) and middle-aged L1 subfamilies (e.g., L1PA2, L1PA3, L1PA4, L1PA5), which are no longer capable of retrotransposition. These findings suggest that the reduced RNA editing activity in senescent cells primarily affects the youngest and most active L1 elements, potentially limiting their mutagenic potential during senescence. This observation aligns with our hypothesis that the activity of APOBEC3 proteins, which are key mediators of L1 RNA editing, is diminished in (pre)senescent cells, thereby contributing to a reduced mutagenic burden in this state.

The reduction of various host factors that inhibit different steps of L1 retrotransposition suggests that L1 elements are not only transcribed, but also translated when cells progress to a senescent state [92]. Indeed, ribosomal profiling analyses demonstrate that L1 ORFs are translated in senescent cells. As we only analyzed retrotransposition-competent copies of full-length L1 elements, the above results suggest that senescent cells are characterized by increased 'jumping' of L1.

Since Alu elements depend on L1 for their transposition and since L1 inhibitors frequently also restrict Alu repeats [93], it is not surprising that expression of the latter is also increased in senescent vs. proliferating cells. Notably, this was not only the case for the youngest and most active sub-subfamily AluY, but also the oldest subfamily AluI.

Since TEs of (pre)senescent cells are derepressed at both the transcriptional and post-transcriptional level, it is tempting to speculate that they promote senescence via two independent mechanisms. First, TE-derived nucleic acids can trigger innate sensing cascades that induce inflammation, IFN secretion and ultimately inflammaging. This proinflammatory cascade has been rigorously documented in the context of aging in murine and human cells [25, 94, 95]. Second, the retrotransposition of L1 and other mobile genetic elements directly induces DNA damage. Since several factors involved in DNA damage repair are downregulated in (pre)senescent cells (e.g. BRCA1, BRCA2, FANCA, FANCD2, etc.), these cells may not be able to repair the damage in a timely manner, which might ultimately lead to a permanent cell-cycle arrest.

Munot et al. Mobile DNA (2025) 16:39 Page 12 of 14

Conclusions

Our findings not only shed light on the differential expression of L1 modulators during the transition of cells to senescence, but also highlight the dual role that TE activation may play in senescence. On the one hand, our study supports a model, in which increased transcription of transposable elements, including L1 and Alu elements, is sensed and triggers IFN-mediated inflammaging. On the other hand, our analysis of Ribo-seq data revealed an increased translation of L1 elements that may enable L1 retrotransposition and ultimately induce genotoxic stress that further promotes transition to senescence. It will be important to decipher the relative contribution of these two mechanisms to senescence. Furthermore, future studies should aim at alleviating the detrimental effects of TEs on cellular senescence, organismal aging and agingassociated diseases. For example, therapeutic approaches that aim at enhancing APOBEC3B activity - or mimicking its antiviral functions - may represent a novel strategy to suppress L1 activity and L1-induced genotoxic stress. Such an approach could be combined with restoring epigenetic silencing of L1 repeats or reverse transcriptase inhibitors to prevent the production of L1-derived nucleic acids triggering detrimental inflammaging.

Abbreviations

A3A Apolipoprotein B mRNA Editing Catalytic Polypeptide-like 3A
A3B Apolipoprotein B mRNA Editing Catalytic Polypeptide-like 3B
A3C Apolipoprotein B mRNA Editing Catalytic Polypeptide-like 3C
A3F Apolipoprotein B mRNA Editing Catalytic Polypeptide-like 3F
A3G Apolipoprotein B mRNA Editing Catalytic Polypeptide-like 3G

ADAR Adenosine Deaminase Acting on RNA

Alu Arthrobacter luteus

APOBEC Apolipoprotein B mRNA Editing Catalytic Polypeptide-like

bps Base pairs
BRCA Breast cancer gene
CPM Counts per million
ES Embryonic stem fibroblasts

EV Empty vector

FANC Fanconi anemia complementation group (FANC)

FPKM Fragments Per Kilobase of transcript per Million mapped reads

GAPDH Glyceraldehyde-3-Phosphate Dehydrogenase

GATK Genome Analysis Toolkit IFI16 Interferon-inducible protein 16

IFN Interferon

L1 Long Interspersed Nuclear Elements-1

KAP1 KRAB-Associated Protein 1

KRAB-ZNF Krüppel-Associated Box Zinc Finger Protein

log2fc Log2 fold change

MCM2 Minichromosome Maintenance Complex Component 2

MOV10 Moloney leukemia virus 10 MPP8 M-Phase Phosphoprotein 8 ORF Open reading frame

qRT-PCR Quantitative Reverse Transcription Polymerase Chain Reaction

RAS^{G12V} Rat sarcoma mutant G12V Ribo-seq Ribosome Profiling Sequencing RNA-seq RNA sequencing

RNASEH2A Ribonuclease H2 Subunit A
SASP Senescence-associated secretory phenotype

SETDB1 Su(var)3-9, Enhancer-of-zeste, and Trithorax Domain Bifurcated

Histone Lysine Methyltransferase 1
SINE Short interspersed nuclear element
TASOR Transcription Activation Suppressor

TE Transposable element

TREX1 Three prime repair exonuclease 1
TRIM28 Tripartite motif-containing protein 28
UCSC University of California, Santa Cruz

UHRF1 Ubiquitin like with PHD and ring finger domains 1

Acknowledgements

The authors would like to thank Thomas Gramberg, Frank Kirchhoff and Terumasa Ikeda for providing the LINE1 reporter constructs, an IFI16 expression vector, and APOBEC3B expression plasmids, respectively. We also thank Prof. Peter Nürnberg and Dr. Vikas Bansal for helpful advice and discussions

Authors' contributions

A.A. conceptualized the study and performed most of the computational analyses. D.M., I.H. and Y.L. performed the qRT-PCR experiments. I.H., Y.L. and C.B. performed the L1 reporter assays. G.N. modified and provided BJ cells. D.S. and C.G. provided resources and acquired funding. A.A., D.S., M.S. and D.M. prepared the figures, and A.A. & M.S. wrote the initial draft of the manuscript. All authors reviewed and edited the manuscript.

Funding

DS was supported by the Heisenberg Program (grant ID: SA 2676/3 – 1) and CRC1506 ("Aging at Interfaces") of the German Research Foundation (DFG).

Data availability

All data generated or analyzed during this study are included in this published article. No new large datasets were generated or uploaded to repositories. The sources of publicly available datasets that were analyzed in the present study are provided in this article.

Declarations

Ethics approval and consent to participate

Not Applicable.

Consent for publication

Not Applicable.

Competing interests

The authors declare no competing interests.

Received: 1 April 2025 / Accepted: 26 September 2025

Published online: 21 October 2025

References

- Mills RE, Bennett EA, Iskow RC, Devine SE. Which transposable elements are active in the human genome? Trends Genet. 2007;23:183–91.
- Kazazian HH Jr, Moran JV. Mobile DNA in health and disease. N Engl J Med. 2017;377:361–70.
- Lander ES, Linton LM, Birren B, Nusbaum C, Zody MC, Baldwin J, et al. Initial sequencing and analysis of the human genome. Nature. 2001;409:860–921.
- Salter JD, Bennett RP, Smith HC. The APOBEC protein family: united by structure, divergent in function. Trends Biochem Sci. 2016;41:578–94.
- Dewannieux M, Esnault C, Heidmann T. LINE-mediated retrotransposition of marked Alu sequences. Nat Genet. 2003;35:41–8.
- Rowe HM, Jakobsson J, Mesnard D, Rougemont J, Reynard S, Aktas T, et al. KAP1 controls endogenous retroviruses in embryonic stem cells. Nature. 2010;463:237–40.
- Seczynska M, Bloor S, Cuesta SM, Lehner PJ. Genome surveillance by HUSHmediated silencing of intronless mobile elements. Nature. 2022;601:440–5.
- Mathavarajah S, Dellaire G. LINE-1: an emerging initiator of cGAS-STING signalling and inflammation that is dysregulated in disease. Biochem Cell Biol. 2024;102:38

 –46.
- Stetson DB, Ko JS, Heidmann T, Medzhitov R. Trex1 prevents cell-intrinsic initiation of autoimmunity. Cell. 2008;134:587–98.
- Liu Q, Yi D, Ding J, Mao Y, Wang S, Ma L, et al. MOV10 recruits DCP2 to decap human LINE-1 RNA by forming large cytoplasmic granules with phase separation properties. EMBO Rep. 2023;24:e56512.

Munot et al. Mobile DNA (2025) 16:39 Page 13 of 14

- Arora R, Bodak M, Penouty L, Hackman C, Ciaudo C. Sequestration of LINE-1 in cytosolic aggregates by MOV10 restricts Retrotransposition. EMBO Rep. 2022;23:e54458.
- Wissing S, Montano M, Garcia-Perez JL, Moran JV, Greene WC. Endogenous APOBEC3B restricts LINE-1 retrotransposition in transformed cells and human embryonic stem cells. J Biol Chem. 2011;286:36427–37.
- 13. Lovsin N, Peterlin BM. Apobec3 proteins inhibit LINE-1 retrotransposition in the absence of ORF1p binding. Ann N Y Acad Sci. 2009;1178:268–75.
- Muckenfuss H, Hamdorf M, Held U, Perković M, Löwer J, Cichutek K, et al. APOBEC3 proteins inhibit human LINE-1 retrotransposition. J Biol Chem. 2006;281:22161–72.
- Stenglein MD, Harris RS. APOBEC3B and APOBEC3F inhibit L1 retrotransposition by a DNA deamination-independent mechanism. J Biol Chem. 2006;281:16837–41.
- Bogerd HP, Wiegand HL, Hulme AE, Garcia-Perez JL, O'Shea KS, Moran JV, et al. Cellular inhibitors of long interspersed element 1 and Alu retrotransposition. Proc Natl Acad Sci U S A. 2006;103:8780–5.
- Richardson SR, Narvaiza I, Planegger RA, Weitzman MD, Moran JV. Apobec3a deaminates transiently exposed single-strand DNA during LINE-1 retrotransposition. Elife. 2014;3:e02008.
- Liang W, Xu J, Yuan W, Song X, Zhang J, Wei W, et al. Apobec3de inhibits LINE-1 retrotransposition by interacting with ORF1p and influencing LINE reverse transcriptase activity. PLoS ONE. 2016;11:e0157220.
- Koyama T, Arias JF, Iwabu Y, Yokoyama M, Fujita H, Sato H, et al. Apobec3g oligomerization is associated with the inhibition of both Alu and LINE-1 retrotransposition. PLoS ONE. 2013;8:e84228.
- Horn AV, Klawitter S, Held U, Berger A, Vasudevan AAJ, Bock A, et al. Human LINE-1 restriction by APOBEC3C is deaminase independent and mediated by an ORF1p interaction that affects LINE reverse transcriptase activity. Nucleic Acids Res. 2014;42:396–416.
- Prior S, Miousse IR, Nzabarushimana E, Pathak R, Skinner C, Kutanzi KR, et al. Densely ionizing radiation affects DNA methylation of selective LINE-1 elements. Environ Res. 2016;150:470–81.
- Singh A, Rappolee DA, Ruden DM. Epigenetic reprogramming in and: from fertilization to primordial germ cell development. Cells. 2023;12. https://doi.org/10.3390/cells12141874.
- Min B, Jeon K, Park JS, Kang Y-K. Demethylation and derepression of genomic retroelements in the skeletal muscles of aged mice. Aging Cell. 2019;18:e13042.
- Ndhlovu LC, Bendall ML, Dwaraka V, Pang APS, Dopkins N, Carreras N, et al. Retro-age: a unique epigenetic biomarker of aging captured by DNA methylation states of retroelements. Aging Cell. 2024;23:e14288.
- De Cecco M, Ito T, Petrashen AP, Elias AE, Skvir NJ, Criscione SW, et al. L1 drives IFN in senescent cells and promotes age-associated inflammation. Nature. 2019;566:73–8.
- Simon M, Van Meter M, Ablaeva J, Ke Z, Gonzalez RS, Taguchi T, et al. LINE1 derepression in aged Wild-Type and SIRT6-Deficient mice drives inflammation. Cell Metab. 2019;29:871–e8855.
- Zarneshan SN, Fakhri S, Bachtel G, Bishayee A. Exploiting pivotal mechanisms behind the senescence-like cell cycle arrest in cancer. Adv Protein Chem Struct Biol. 2023;135:1–19.
- Kumari R, Jat P. Mechanisms of cellular senescence: cell cycle arrest and senescence associated secretory phenotype. Front Cell Dev Biol. 2021 0 645 F23
- Brégnard C, Guerra J, Déjardin S, Passalacqua F, Benkirane M, Laguette N. Upregulated LINE-1 activity in the Fanconi anemia cancer susceptibility syndrome leads to spontaneous pro-inflammatory cytokine production. EBioMedicine. 2016;8:184–94.
- 30. da Silva PFL, Ogrodnik M, Kucheryavenko O, Glibert J, Miwa S, Cameron K, et al. The bystander effect contributes to the accumulation of senescent cells in vivo. Aging Cell. 2019;18:e12848.
- Ramini D, Latini S, Giuliani A, Matacchione G, Sabbatinelli J, Mensà E, et al. Replicative senescence-associated LINE1 methylation and LINE1-Alu expression levels in human endothelial cells. Cells. 2022. https://doi.org/10.3390/cells11233799
- Tang H, Yang J, Xu J, Zhang W, Geng A, Jiang Y, et al. The transcription factor PAX5 activates human LINE1 retrotransposons to induce cellular senescence. EMBO Rep. 2024;25:3263–75.
- 33. Loayza-Puch F, Drost J, Rooijers K, Lopes R, Elkon R, Agami R. p53 induces transcriptional and translational programs to suppress cell proliferation and growth. Genome Biol. 2013;14:R32.

- 34. Dobin A, Davis CA, Schlesinger F, Drenkow J, Zaleski C, Jha S, et al. STAR: ultrafast universal RNA-seq aligner. Bioinformatics. 2013;29:15–21.
- Liao Y, Smyth GK, Shi W. Featurecounts: an efficient general purpose program for assigning sequence reads to genomic features. Bioinformatics. 2014;30:923–30.
- Liu N, Lee CH, Swigut T, Grow E, Gu B, Bassik MC, et al. Selective Silencing of euchromatic L1s revealed by genome-wide screens for L1 regulators. Nature. 2018;553:228–32.
- Frassinelli L, Orecchini E, Al-Wardat S, Tripodi M, Mancone C, Doria M, et al. The RNA editing enzyme ADAR2 restricts L1 mobility. RNA Biol. 2021;18:75–87.
- Orecchini E, Doria M, Antonioni A, Galardi S, Ciafrè SA, Frassinelli L, et al. ADAR1 restricts LINE-1 retrotransposition. Nucleic Acids Res. 2017;45:155–68.
- Bulliard Y, Narvaiza I, Bertero A, Peddi S, Röhrig UF, Ortiz M, et al. Structurefunction analyses point to a polynucleotide-accommodating groove essential for APOBEC3A restriction activities. J Virol. 2011;85:1765–76.
- Miyoshi T, Makino T, Moran JV. Poly(ADP-Ribose) polymerase 2 recruits replication protein A to sites of LINE-1 integration to facilitate Retrotransposition. Mol Cell. 2019;75:1286–e129812.
- Mitra M, Hercík K, Byeon I-JL, Ahn J, Hill S, Hinchee-Rodriguez K, et al. Structural determinants of human APOBEC3A enzymatic and nucleic acid binding properties. Nucleic Acids Res. 2014;42:1095–110.
- Khatua AK, Taylor HE, Hildreth JEK, Popik W. Inhibition of LINE-1 and Alu retrotransposition by exosomes encapsidating APOBEC3G and APOBEC3F. Virology. 2010;400:68–75.
- 43. Carugno M, Maggioni C, Crespi E, Bonzini M, Cuocina S, Dioni L, et al. Night shift work, DNA methylation and telomere length: an investigation on hospital female nurses. Int J Environ Res Public Health. 2019. https://doi.org/10.3390/jjerph16132292.
- Ketola K, Kaljunen H, Taavitsainen S, Kaarijärvi R, Järvelä E, Rodríguez-Martín B, et al. Subclone eradication analysis identifies targets for enhanced cancer therapy and reveals L1 retrotransposition as a dynamic source of cancer heterogeneity. Cancer Res. 2021;81:4901–9.
- 45. Bamberger C, Pankow S, Yates JR 3. rd. SMG1 and CDK12 link Δ Np63 α phosphorylation to RNA surveillance in keratinocytes. J Proteome Res. 2021;20:5347–58.
- Bona N, Crossan GP. Fanconi anemia DNA crosslink repair factors protect against LINE-1 retrotransposition during mouse development. Nat Struct Mol Biol. 2023;30:1434–45.
- Servant G, Streva VA, Derbes RS, Wijetunge MI, Neeland M, White TB, et al. The nucleotide excision repair pathway limits L1 retrotransposition. Genetics. 2017;205:139–53.
- Gasior SL, Roy-Engel AM, Deininger PL. ERCC1/XPF limits L1 retrotransposition. DNA Repair. 2008;7:983–9.
- Tristan-Ramos P, Morell S, Sanchez L, Toledo B, Garcia-Perez JL, Heras SR. sRNA/L1 retrotransposition: using siRNAs and miRNAs to expand the applications of the cell culture-based LINE-1 retrotransposition assay. Philos Trans R Soc Lond B Biol Sci. 2020;375:20190346.
- Xu B, Li X, Zhang S, Lian M, Huang W, Zhang Y, et al. Pan cancer characterization of genes whose expression has been associated with LINE-1 antisense promoter activity. Mob DNA. 2023;14:13.
- Simbolo M, Bilotta M, Mafficini A, Luchini C, Furlan D, Inzani F, et al. Gene expression profiling of pancreas neuroendocrine tumors with different Ki67based grades. Cancers (Basel). 2021. https://doi.org/10.3390/cancers13092054.
- Pandiloski N, Horváth V, Karlsson O, Koutounidou S, Dorazehi F, Christoforidou G, et al. DNA methylation governs the sensitivity of repeats to restriction by the HUSH-MORC2 corepressor. Nat Commun. 2024;15:7534.
- Goodier JL, Wan H, Soares AO, Sanchez L, Selser JM, Pereira GC, et al. ZCCHC3 is a stress granule zinc knuckle protein that strongly suppresses LINE-1 retrotransposition. PLoS Genet. 2023;19:e1010795.
- Jensvold ZD, Christenson AE, Flood JR, Lewis PW. Interplay between two paralogous human Silencing hub (HuSH) complexes in regulating LINE-1 element Silencing. BioRxiv. 2024. https://doi.org/10.1101/2023.12.28.573526.
- Douse CH, Tchasovnikarova IA, Timms RT, Protasio AV, Seczynska M, Prigozhin DM, et al. TASOR is a pseudo-PARP that directs HUSH complex assembly and epigenetic transposon control. Nat Commun. 2020;11:4940.
- Choi J, Hwang S-Y, Ahn K. Interplay between RNASEH2 and MOV10 controls LINE-1 retrotransposition. Nucleic Acids Res. 2018;46:1912–26.
- Pokatayev V, Hasin N, Chon H, Cerritelli SM, Sakhuja K, Ward JM, et al. RNase H2 catalytic core Aicardi-Goutières syndrome-related mutant invokes cGAS-STING innate immune-sensing pathway in mice. J Exp Med. 2016;213:329–36.

Munot et al. Mobile DNA (2025) 16:39 Page 14 of 14

- Robbez-Masson L, Tie CHC, Conde L, Tunbak H, Husovsky C, Tchasovnikarova IA, et al. The HUSH complex cooperates with TRIM28 to repress young retrotransposons and new genes. Genome Res. 2018;28(6):836–45.
- Volkmann B, Wittmann S, Lagisquet J, Deutschmann J, Eissmann K, Ross JJ, et al. Human TRIM5α senses and restricts LINE-1 elements. Proc Natl Acad Sci U S A. 2020;117:17965–76.
- Ding J, Wang S, Liu Q, Duan Y, Cheng T, Ye Z, et al. Schlafen-5 inhibits LINE-1 retrotransposition. iScience. 2023;26:107968.
- Xiong F, Wang R, Lee J-H, Li S, Chen S-F, Liao Z, et al. RNA mA modification orchestrates a LINE-1-host interaction that facilitates retrotransposition and contributes to long gene vulnerability. Cell Res. 2021;31:861–85.
- Fernandes LP, Enriquez-Gasca R, Gould PA, Holt JH, Conde L, Ecco G, et al. A satellite DNA array barcodes chromosome 7 and regulates totipotency via ZFP819. Sci Adv. 2022;8:eabp8085.
- Müller I, Moroni AS, Shlyueva D, Sahadevan S, Schoof EM, Radzisheuskaya A, et al. MPP8 is essential for sustaining self-renewal of ground-state pluripotent stem cells. Nat Commun. 2021;12:3034.
- Healton SE, Pinto HD, Mishra LN, Hamilton GA, Wheat JC, Swist-Rosowska K, et al. H1 linker histones silence repetitive elements by promoting both histone H3K9 methylation and chromatin compaction. Proc Natl Acad Sci U S A. 2020:117:14251–8.
- Fukuda K, Shinkai Y. Setdb1-mediated silencing of retroelements. Viruses. 2020. https://doi.org/10.3390/v12060596.
- Jurkowska RZ, Qin S, Kungulovski G, Tempel W, Liu Y, Bashtrykov P, et al. H3K14ac is linked to methylation of H3K9 by the triple Tudor domain of SETDB1. Nat Commun. 2017;8:2057.
- 67. Danac JMC, Matthews RE, Gungi A, Qin C, Parsons H, Antrobus R, et al. Competition between two HUSH complexes orchestrates the immune response to retroelement invasion. Mol Cell. 2024;84:2870–e28815.
- Li Z, Duan S, Hua X, Xu X, Li Y, Menolfi D, et al. Asymmetric distribution of parental H3K9me3 in S phase silences L1 elements. Nature. 2023;623:643–51.
- 69. Langmead B, Salzberg SL. Fast gapped-read alignment with bowtie 2. Nat Methods. 2012;9:357–9.
- Trapnell C, Williams BA, Pertea G, Mortazavi A, Kwan G, van Baren MJ, et al. Transcript assembly and quantification by RNA-Seq reveals unannotated transcripts and isoform switching during cell differentiation. Nat Biotechnol. 2010;28:511–5.
- Kent WJ, Sugnet CW, Furey TS, Roskin KM, Pringle TH, Zahler AM, et al. The human genome browser at UCSC. Genome Res. 2002;12:996–1006.
- McKenna A, Hanna M, Banks E, Sivachenko A, Cibulskis K, Kernytsky A, et al. The genome analysis toolkit: a mapreduce framework for analyzing nextgeneration DNA sequencing data. Genome Res. 2010;20:1297–303.
- Piskol R, Ramaswami G, Li JB. Reliable identification of genomic variants from RNA-seq data. Am J Hum Genet. 2013;93:641–51.
- 74. Quinlan AR, Hall IM. BEDTools: a flexible suite of utilities for comparing genomic features. Bioinformatics. 2010;26:841–2.
- Kim D, Pertea G, Trapnell C, Pimentel H, Kelley R, Salzberg SL. Tophat2: accurate alignment of transcriptomes in the presence of insertions, deletions and gene fusions. Genome Biol. 2013;14:R36.
- Ramírez F, Dündar F, Diehl S, Grüning BA, Manke T. DeepTools: a flexible platform for exploring deep-sequencing data. Nucleic Acids Res. 2014;42:W187-91.
- Ostertag EM, Prak ET, DeBerardinis RJ, Moran JV, Kazazian HH Jr. Determination of L1 Retrotransposition kinetics in cultured cells. Nucleic Acids Res. 2000;28:1418–23.

- Hotter D, Bosso M, Jønsson KL, Krapp C, Stürzel CM, Das A, et al. IFI16 targets the transcription factor Sp1 to suppress HIV-1 transcription and latency reactivation. Cell Host Microbe. 2019;25:858–e87213.
- Meessen S, Najjar G, Azoitei A, Iben S, Bolenz C, Günes C. A comparative assessment of replication stress markers in the context of telomerase. Cancers (Basel). 2022;14. https://doi.org/10.3390/cancers14092205.
- 80. Meena J, Rudolph KL, Günes C. Telomere Dysfunction, chromosomal instability and cancer. Recent results in cancer Research. Fortschritte der krebsforschung. Progres Dans Les Recherches Sur Le Cancer. 2015;200:61–79.
- Zhou J, Liu K, Bauer C, Bendner G, Dietrich H, Slivka JP, et al. Modulation of cellular senescence in HEK293 and HepG2 cells by ultrafiltrates Upla and Ulu is partly mediated by modulation of mitochondrial homeostasis under oxidative stress. Int J Mol Sci. 2023. https://doi.org/10.3390/ijms24076748.
- 82. Turelli P, Castro-Diaz N, Marzetta F, Kapopoulou A, Raclot C, Duc J, et al. Interplay of TRIM28 and DNA methylation in controlling human endogenous retroelements. Genome Res. 2014;24:1260–70.
- Orecchini E, Frassinelli L, Galardi S, Ciafrè SA, Michienzi A. Post-transcriptional regulation of LINE-1 retrotransposition by AID/APOBEC and ADAR deaminases. Chromosoma Res. 2018;26:45–59.
- 84. Jurka J, Smith T. A fundamental division in the Alu family of repeated sequences. Proc Natl Acad Sci U S A. 1988;85:4775–8.
- 85. Batzer MA, Deininger PL, Hellmann-Blumberg U, Jurka J, Labuda D, Rubin CM, et al. Standardized nomenclature for Alu repeats. J Mol Evol. 1996;42:3–6.
- Sanchez A, Ortega P, Sakhtemani R, Manjunath L, Oh S, Bournique E, et al. Mesoscale DNA features impact APOBEC3A and APOBEC3B deaminase activity and shape tumor mutational landscapes. Nat Commun. 2024;15:2370.
- Savva YA, Rieder LE, Reenan RA. The ADAR protein family. Genome Biol. 2012;13:252.
- 88. Choudhary S, Li W, D Smith A. Accurate detection of short and long active ORFs using Ribo-seq data. Bioinformatics. 2020;36:2053–9.
- Doehle BP, Schäfer A, Cullen BR. Human APOBEC3B is a potent inhibitor of HIV-1 infectivity and is resistant to HIV-1 Vif. Virology. 2005;339:281–8.
- Kinomoto M, Kanno T, Shimura M, Ishizaka Y, Kojima A, Kurata T, et al. All APO-BEC3 family proteins differentially inhibit LINE-1 retrotransposition. Nucleic Acids Res. 2007;35:2955–64.
- Covino DA, Gauzzi MC, Fantuzzi L. Understanding the regulation of APOBEC3 expression: current evidence and much to learn. J Leukoc Biol. 2018;103:433–44.
- 92. Rosser JM, An W. L1 expression and regulation in humans and rodents. Front Biosci (Elite Ed). 2012;4:2203–25.
- 93. Stenz L.The L1-dependant and pol III transcribed Alu retrotransposon, from its discovery to innate immunity. Mol Biol Rep. 2021;48:2775–89.
- Reid Cahn A, Bhardwaj N, Vabret N. Dark genome, bright ideas: recent approaches to harness transposable elements in immunotherapies. Cancer Cell. 2022;40:792–7.
- 95. Gazquez-Gutierrez A, Witteveldt J, Heras R, Macias S. Sensing of transposable elements by the antiviral innate immune system. RNA. 2021;27(7):735–52.

Publisher's note

Springer Nature remains neutral with regard to jurisdictional claims in published maps and institutional affiliations.